

Localization effects in Co- and Ni-doped $\text{Bi}_2\text{Sr}_2\text{CaCu}_2\text{O}_{8+y}$

C. Quitmann*

Department of Physics, University of Wisconsin, Madison, Wisconsin 53706

P. Almeras

Institute de Physique Appliqué, Ecole Polytechnique Federale, CH-1015 Lausanne, Switzerland

Jian Ma and R. J. Kelley

Department of Physics, University of Wisconsin, Madison, Wisconsin 53706

H. Berger

Institute de Physique Appliqué, Ecole Polytechnique Federale, CH-1015 Lausanne, Switzerland

Cai Xueyu

Institut for Applied Superconductivity, University of Wisconsin, Madison, Wisconsin 53706

G. Margaritondo

Institute de Physique Appliqué, Ecole Polytechnique Federale, CH-1015 Lausanne, Switzerland

M. Onellion

Department of Physics, University of Wisconsin, Madison, Wisconsin 53706

(Received 20 July 1995)

We have studied the influence of Co and Ni doping on the electronic band structure and the transport properties of high-temperature superconductors. The doping has dramatic effects on both the normal and the superconducting state. Upon doping the residual resistivity increases strongly. For sufficiently high Co concentration the temperature dependence $\rho(T)$ turns from a simple linear dependence to one displaying a minimum around $T_{\min}=190$ K. This minimum is followed by an upturn ($d\rho/dT<0$) and by a transition to a superconducting state at even lower temperature ($T_c=66$ K). These changes in the resistivity are accompanied by an almost complete disappearance of the dispersing bandlike states in angle-resolved photoemission. We show that spatial localization of the carrier states through the doping-induced disorder provides a consistent explanation of the experimental results. However, none of the standard scattering mechanisms can explain the observed localization. Because the increase in the residual resistivity is higher than the unitary limit, the localization has to be through a cooperative effect. This rules out standard Abrikosov-Gor'kov or Kondo effects. We discuss the observed coexistence of localization and superconductivity in terms of the relevant length scales and compare it to theoretical predictions.

INTRODUCTION

High-temperature superconductors (HTSC) are well known to be close to a superconductor-insulator transition¹⁻⁵ that can be achieved by cation doping. However, the nature of this transition is not well understood. Particularly puzzling are the results of transition-metal doping. Doping with both magnetic (Fe, Co, and Ni) and nonmagnetic (Zn) $3d$ ions suppresses superconductivity and leads to a superconductor-insulator transition.³ While magnetic impurities are known to suppress T_c due to Abrikosov-Gor'kov pair breaking,^{6,7} Anderson's theorem⁸ states that nonmagnetic impurities should not affect T_c at all. Furthermore, at the percent doping level the scattering processes from impurities are expected to be independent and thus cannot be expected to lead to a transition from metallic ($d\rho/dT>0$) to insulating ($d\rho/dT<0$) behavior. In this paper, we combine measurements of the electrical resistivity $\rho_{ab}(T)$ with angle-resolved photoemission experiments (ARUPS) which investigate the dis-

persing band states $E(k)$. This combination gives new insight into the influence of doping on the electronic structure. We show that the metal-insulator transition in HTSC is different from that observed previously in low-temperature superconductors and does not fit any standard model. Superconductor-insulator transitions have long been studied in low-temperature superconductors.⁹⁻¹¹ Here two cases can be distinguished: homogenous ultrathin films (Pb) (Ref. 12) and granular cluster systems ($\text{Al}_{1-x}\text{Ge}_x$).¹³ In both cases, one starts from a superconducting ground state described by a macroscopic wave function $\Psi(r)=\Psi_0\exp(i\cdot\varphi)$. When approaching the superconductor-insulator transition by varying either the film thickness (homogenous case) or the metal to nonmetal fraction (granular case), this macroscopic wave function is destroyed. In homogenous systems, this happens through scattering processes which reduce the amplitude Ψ_0 and thus the density of Cooper pairs $n_c=|\Psi_0|^2$. These scattering processes lead to a continuous decrease of the transition temperature T_c and the superconducting gap Δ with in-

creasing disorder, i.e., decreased film thickness.^{14,15} In contrast, the granular systems are characterized by destruction of the phase coherence between superconducting clusters leading to a spatial variation in the phase, $\varphi = \varphi(r)$. In these granular systems the T_c is given by the T_c of the metallic clusters, which is independent of the metal to nonmetal fraction. Thus the onset of the superconducting transition is independent of composition. The transition width, however, increases as the superconductor-insulator transition is approached due to the percolative nature of the system.

By combining angle-resolved photoemission (ARUPS) with measurements of the electrical resistivity $\varrho_{ab}(T)$ we are able to relate changes in the transport properties to changes in the electronic structure. Our findings are threefold. First, we confirm that the doping affects not only the superconducting, but also the normal state and thus cannot be discussed in a simple Abrikosov-Gor'kov scheme. These results are confirmed by previously published work.³ Second, we show that the metal-insulator transition seen in the transport measurements correlates with the suppression of dispersing bandlike states. Third, we show that some samples show superconductivity even though their normal state is insulating ($d\varrho/dT < 0$). We argue that this indicates that in HTSC Cooper pairs can be formed out of carriers that are almost localized in the normal state. We show that the assumption of spatial localization of the carriers through the disorder introduced by the transition-metal doping provides a consistent explanation of a variety of experimental facts. When using the term *localization* we do not imply localization through quantum interference as seen in weak localization.¹⁶ We use it in a more general sense, meaning that the spatial extent, or the mean free path λ of the electronic carrier states is comparable or smaller than their separation d_{e-e} .

The idea that the superconductor-insulator transition in HTSC is caused by disorder has previously been suggested by different authors^{4,5,17,18} and transport measurements like those reported here have also been reported by several other groups.^{3,4,19,20} This is a report linking the changes observed in the resistivity to changes in the electronic dispersion, and we establish the coexistence of localization and superconductivity in a homogenous system such as the HTSC's. Previously, coexistence of localization and superconductivity has only been observed in granular systems^{13,21} for which there are also numerous theoretical studies.²²⁻²⁵

This investigation was conducted on the HTSC $\text{Bi}_2\text{Sr}_2\text{CaCu}_2\text{O}_{8+y}$ (Bi-2212) doped with either Co or Ni. This system is known to exhibit a superconductor-insulator transition,³ and there is theoretical evidence that disorder effects are much stronger in HTSC's than in conventional metals.²⁶⁻²⁸ Both, Co and Ni act as impurities because their electronic structure and size differs from that of the Cu ions they replace. This perturbs the periodic potential of the CuO_2 plane.

In a previous report Rong Liu and co-workers have investigated the band structure of $\text{YBa}_2\text{Cu}_3\text{O}_x$ as a function of the oxygen content with $6.3 \leq x \leq 6.9$.^{29,30} Here the change in the oxygen content is expected to lead to a change in the carrier density and thus to changes in the Fermi surface. The experiments however only show relatively small changes in the Fermi surface for metallic samples ($x=6.9$ and $x=6.5$). For an insulating sample the authors observed a significant de-

crease of spectral weight for the dispersing states. We will compare our results to those on $\text{YBa}_2\text{Cu}_3\text{O}_x$ in the discussion section.

HTSC's are well suited for this investigation because, due to their layered structure, their electronic structure is quasi-two-dimensional. Experimentally, one observes a semiconducting resistivity ($d\varrho_c/dT < 0$) for the resistivity along the c axis, while the resistivity is metallic in the ab plane ($d\varrho_{ab}/dT > 0$). The resistivity anisotropy is about $\varrho_c/\varrho_{ab} \cong 10^4$ for the carrier concentration used here.³¹ Electronic screening is known to be reduced in two-dimensional systems and thus effects of impurities are expected to be particularly strong in this material.

The impurity concentrations used in this study are below about 3 at. %. Assuming that Co and Ni substitute randomly for Cu, the separation between impurities ($\sim 30 \text{ \AA}$ at 3 at. %) is much larger than their diameter ($\sim 1 \text{ \AA}$). We are thus well below the percolation threshold in two dimensions and can expect to be in the homogenous limit. Because of the large separation between the impurities there is *a priori* no reason for not treating the scattering in a single impurity picture. In the following, we will however show that a single impurity picture is inappropriate and that cooperative effects need to be considered. If the impurities were not distributed randomly but were clustered, this would reduce their influence on the transport and thus cannot explain the observed effects.

The structure of the paper is as follows. After explaining the experimental details we will first show the influence of Co doping on the electrical resistivity and then on the dispersing electronic states. After this, we will show results of Ni doping as a comparison. This section will be followed by the analysis of the data in terms of localization through disorder and by the conclusions.

EXPERIMENTAL

The single crystals were grown by the conventional self-flux method. Their composition was determined with electronprobe microanalysis (EPMA) (Cameca CAMEBAX SX-50). Their size is typically $2 \times 2 \times 0.05 \text{ mm}^3$. Using the self-flux method we observe a solubility limit for Co and Ni in Bi-2212 of around 2–3 at. %. Above this level the transition metals are no longer incorporated in the crystals. Thus we were unable to investigate samples with higher transition metal concentration.

We report on measurements of four samples, one undoped reference sample, two Co-doped samples and one Ni-doped sample. The Co-doped samples have Co contents, as determined by EPMA, of $c_{\text{Co}} = 1.57 \text{ at. \%}$ and $c_{\text{Co}} = 1.60 \text{ at. \%}$. Given the uncertainty of the EPMA measurement of $\sim 0.3 \text{ at. \%}$ the samples have almost the same Co content. However, their resistivity and electronic structure are very different. In the following they will be called sample No. 1 ($c_{\text{Co}} = 1.57 \text{ at. \%}$) and sample No. 2 ($c_{\text{Co}} = 1.60 \text{ at. \%}$), respectively. The Ni-doped sample has a Ni content of about $c_{\text{Ni}} = 3 \text{ at. \%}$.

Angle-resolved photoemission (ARUPS) experiments were performed at the $4m$ normal incidence monochromator (4m-NIM) of the Synchrotron Radiation Center in Stoughton, Wisconsin with a photon energy of 21 eV. After cleaving the samples in UHV ($p < 1 \times 10^{-10} \text{ torr}$) low-energy electron diffraction was performed *in situ* to check the surface quality

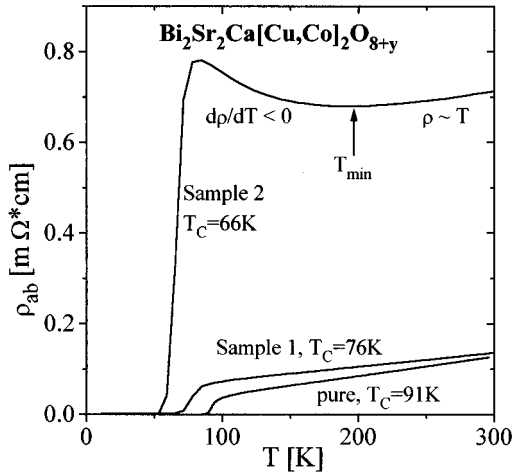


FIG. 1. Electrical resistivity in the a,b plane $\rho_{ab}(T)$ for a pure Bi-2212 sample and two samples with 1.57 at. % Co (No. 1) and 1.60 at. % Co (No. 2), respectively. Note the suppression of T_c and the transition to insulating behavior ($d\rho/dT < 0$) with increasing Co doping.

and the orientation of the sample. The samples were oriented with the a axis (Γ - X) parallel to the photon electric field. For the Bi-2212 system this is the direction of the Bi-O bond which does not show the superlattice modulation³¹⁻³³ and it is at 45° to the Cu-O-Cu bond direction (Γ - M). Because of the symmetry of the normal state this geometry favors the observation of the dispersing band state along the Γ - X direction but reduces photoemission from the states along Γ - M .³⁴ The spectra for the pure reference material were taken at $T=100$ K with a combined resolution of 35 meV, as determined from the 10 to 90 % value of the Fermi edge of a Au film situated next to the sample. The spectra of the doped samples were taken at room temperature with a combined energy resolution of 120 meV. The photon angle of incidence was 45° . All angles are measured with respect to the surface normal. The binding energies of all spectra are referred to the Fermi energy of a Au film located next to the sample and electrically connected to it. All spectra shown are normalized to the intensity at 0.85 eV binding energy.

Resistivity measurements were performed on the same samples after taking them out of the photoemission chamber. Current and voltage leads were attached by silver epoxy onto the a,b plane of the crystals to measure the a,b -plane resistivity, $\rho_{ab}(T)$. Due to the irregular shape of the crystals after cleavage the absolute values of the resistivity are only approximate.

RESULTS

A. Electrical resistivity of Co-doped Bi-2212

Figure 1 illustrates the electrical resistivity $\rho_{ab}(T)$ of a pure Bi-2212 and the two doped samples No. 1 ($c_{Co}=1.57$ at. %) and No. 2 ($c_{Co}=1.60$ at. %). The pure sample shows the well known linear resistivity $\rho_{ab}(T) = \rho_0 + a \cdot T$.³⁵ A simple linear extrapolation of the resistivity between 300 and 120 K yields a vanishing residual resistivity. The midpoint of the superconducting transition is $T_{c,mid}=91$ K. The sample with the lower Co content (No. 1) still shows a resistivity linear in temperature but with a rather high residual resistiv-

ity of $\rho_0(\text{No. 1})=43 \mu\Omega \text{ cm}$. This large residual resistivity indicates a decreased mean free path λ caused by scattering from the Co impurities. At $T=100$ K the resistivity is a factor of 2 higher than for the pure sample. For sample No. 2 we observe a qualitative change. The resistivity at room temperature has increased by a factor of 6 compared to the pure sample. Even more important, after decreasing slightly ($d\rho/dT > 0$) on going to lower temperatures it shows a minimum at $T_{min}=190$ K and then *increases* towards lower temperatures ($d\rho/dT < 0$). At still lower temperatures, we observe a superconducting transition with $T_{c,mid}=66$ K. The negative temperature coefficient ($d\rho/dT < 0$) of the electrical resistivity between $T_{min}=190$ K and T_c is a clear indication of insulating behavior caused by localization of the charge carriers. The residual resistivity for this sample is about $\rho_0(\text{No. 2}) \sim 600 \mu\Omega \text{ cm}$. While a positive temperature coefficient ($d\rho/dT > 0$) indicates scattering of delocalized states by thermal excitations, a negative temperature coefficient ($d\rho/dT < 0$) indicates either the presence of a gap in the electronic structure, or spatial localization of the electronic states. In the latter case transport can occur by hopping between such localized states.³⁶ As will be shown later the hopping process is the most likely case in these samples. The negative temperature coefficient is thus the first indication of disorder-induced spatial localization.

In the temperature range between T_c and T_{min} the charge carriers are transported through thermally activated hopping between localized single-particle sites.³⁶ Such hopping processes are frozen out as the temperature decreases because the thermal energy available to hop to an empty site becomes smaller. Above T_{min} the thermal energy is sufficient to excite the carriers across the mobility gap into delocalized states.⁵ Therefore the size of the mobility gap in this sample is roughly $\Delta E_{mob} \sim k_B \cdot T_{min} = k_B \cdot 190$ K or 16 meV.

It is important to realize that the minimum in the resistivity cannot be explained by sample inhomogeneities. An inhomogeneous sample results in a parallel resistor network of insulating and a metallic (superconducting) material. In such a parallel network, the resistivity is dominated by the component with the lower resistivity. Thus a parallel network of resistors cannot account for the observed minimum. Because the experiments were done on single crystals, grain boundaries can also be excluded as a possible origin of the minimum in $\rho_{ab}(T)$.

The Co doping affects not only the normal state but also the transition temperature T_c . It decreases from $T_c=91$ K in the pure material to $T_c=76$ K in sample No. 1 and $T_c=66$ K in sample No. 2. This decrease of T_c is a characteristic feature of homogenous systems.^{9,11} If the system was inhomogeneous one would expect the granular superconducting regions to have the same T_c as the pure material. Only their coupling would be perturbed because of intermediate nonsuperconducting regions. This would lead to a broadening of the transition but leave the onset virtually unchanged. The Co-doped Bi-2212 is therefore in the homogenous limit of a superconductor-insulator transition.

It is informative to compare our results to photodoping experiments.^{18,37,38} In our study we have changed the disorder by doping without significantly affecting the carrier density. Our results indicate a homogenous system with a decreasing T_c . In the photodoping experiments the sample is

exposed to laser pulses which can create photoinduced carriers. Their number depends on the laser power and wavelength.^{18,37} Thus in photodoping experiments the carrier density can be changed without significantly changing the disorder. In these experiments one observes superconductivity which is induced by the illumination. But in contrast to our results the onset of the superconducting transition $T_{c,on}$ is constant. It is not dependent on the illuminating power. The width of the transition, on the other hand, decreases monotonically with illuminating power. Thus these experiments indicate a granular system. These apparently contradicting results indicate that there is a real lack in the understanding of localization in these systems. We return to this question below.

The relative decrease of T_c between the pure Bi-2212 and sample No. 1 is $\Delta T_c/\Delta c \sim 9$ K/at. %. Between sample No. 1 and sample No. 2 the reduction is much stronger, at least: $\Delta T_c/\Delta c > 30$ K/at. %. The initial suppression rate is comparable to the suppression observed in polycrystalline material which is ~ 6 K/at. % for Co and for Zn.³ The drastic decrease of T_c on going from the metallic sample No. 1 to the insulating sample No. 2 is what one would expect when the Fermi energy crosses the mobility edge and reaches the region where the single-particle excitations are localized.²² This is therefore the second indication of localization through doping induced disorder.

The coexistence of superconductivity and localization has so far only been seen in granular low- T_c systems such as $Al_{1-x}Ge_x$ (Ref. 13) and $In_{1-x}O_x$.²¹ Disordered HTSC samples are the first to show such a coexistence in a homogeneous material. This is of particular interest for theoretical models because it shows that even in the situation where the single-particle excitations are almost localized, the attractive interaction persists and is not completely overwhelmed by the poorly screened Coulomb repulsion. Therefore, the assumption of the existence of a pairing interaction even in the insulating phase remains a reasonable starting point for theoretical models of the superconductor-insulator transition.

B. Angle-resolved photoemission

Figures 2, 3, and 4 illustrate ARUPS spectra for the identical three Co-doped samples as in Fig. 1. We show spectra along two main symmetry directions Γ - M (Cu-O-Cu bond direction) and Γ - X (a axis, 45° to Γ - M). The spectra are comprised of three contributions: a decaying background (caused by the valence band located at about 3 eV binding energy); a relatively broad (full width at half maximum ~ 200 meV) dispersing state of Lorentzian shape, and elastically scattered electrons forming a Fermi-Dirac distribution. A decomposition into these three contributions will be shown later in Fig. 7. In the following, we will focus on the dispersing band because it provides information about the delocalized states.

In the undoped sample (Fig. 2) the dispersing band is strong along the Γ - X direction. The band becomes visible above the background at $\theta=8^\circ$, then disperses towards the Fermi energy E_F and crosses it around $\theta=14^\circ$. This crossing point of the band is important because it indicates the size of the Fermi surface. In the absence of changes in the topology, which are not expected to be caused by doping at this low level, the crossing point is directly related to the carrier den-

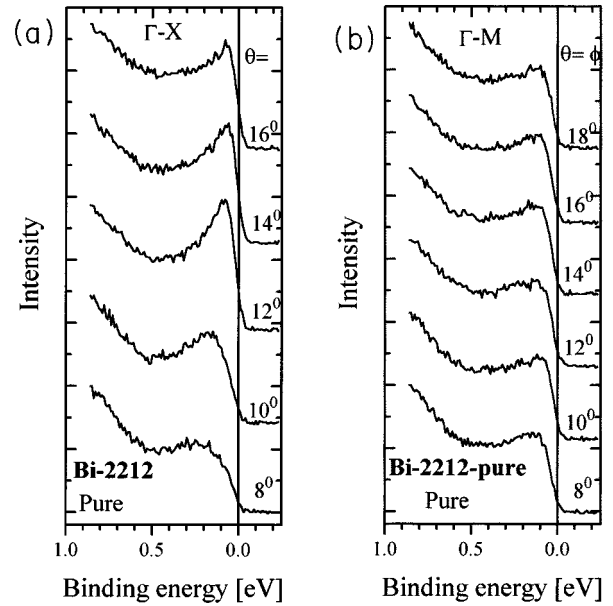


FIG. 2. ARUPS spectra for a pure Bi-2212 single crystal. The momentum of the photoelectron is parallel to the a axis (Γ - X) in (a) and parallel to the Cu-O-Cu bond (Γ - M) in (b). The spectra clearly show a peak which disperses with increasing angle. Along the Γ - X direction it cuts the Fermi surface around $\theta=14^\circ$.

sity. Along the Γ - M direction we also observe a dispersing state but its intensity is weaker. The band disperses towards E_F and then remains close, but below, E_F for a significant portion of the zone.^{39,40} This extended region with almost no dispersion causes a near singularity in the density of states along the Γ - M direction, similar to earlier reports on $YBa_2Cu_3O_{7-x}$.^{41,42} As a result, the density of states is very high along this direction.

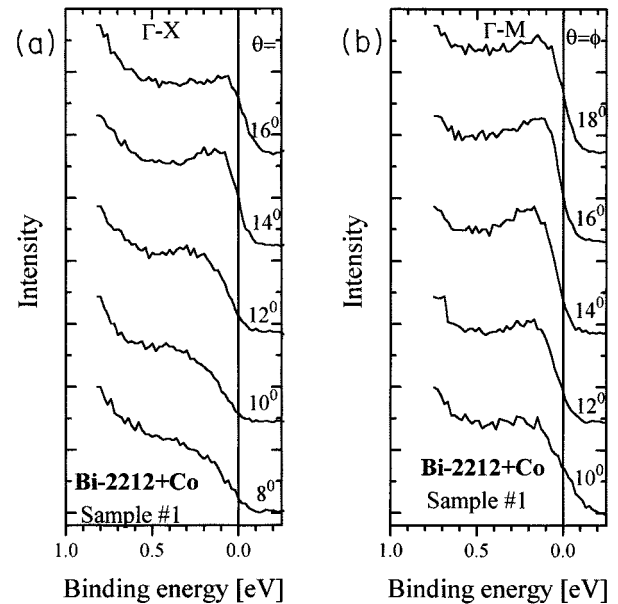


FIG. 3. ARUPS spectra for a Co-doped Bi-2212 single crystal (sample No. 1). The orientation is identical to that in Fig. 2. Compared to the pure crystal in Fig. 1 the intensity of the dispersing state along Γ - X is strongly reduced. However the crossing point is still around $\theta=14^\circ$.

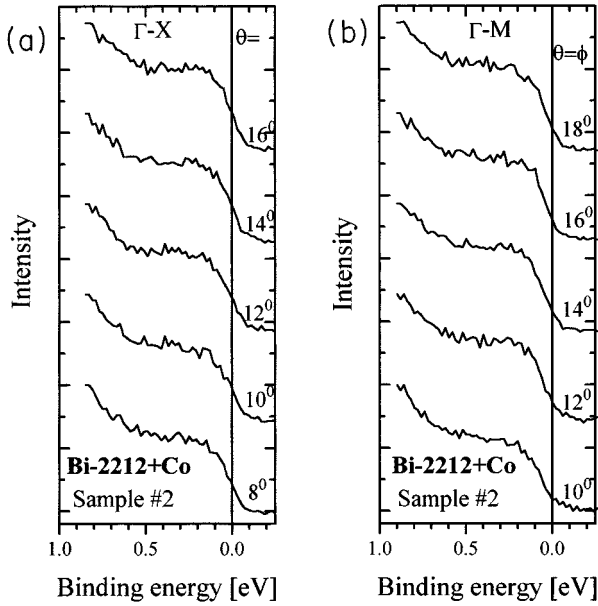


FIG. 4. ARUPS spectra for Co-doped Bi2212 single crystal (sample No. 2). The orientation is identical to that in Fig. 2. This sample showed the insulating upturn in the resistivity in Fig. 1. The dispersing state has virtually disappeared along both directions.

The data for the Co-doped sample No. 1 are illustrated in Fig. 3. Along Γ -X we also observe a dispersing bandlike state, although its intensity is significantly reduced compared to the pure sample in Fig. 2(a). The dispersion is, within the error bars, identical to that of the undoped sample. The band crosses the Fermi surface at $\theta=14^\circ$, the same location as for the pure sample. This indicates an unchanged carrier concentration. In fact, because Co is a $2+$ ion such a change would not be expected. Hall-effect data also indicate that there is no change in the carrier concentration.³

For the Γ -M direction the spectra in Fig. 3(b) are similar to those of the pure sample in Fig. 2(b). The intensity of the dispersing state has decreased only slightly and the band still shows a dispersion towards the Fermi surface, without crossing it. There is less reduction in intensity of the bandlike state in the Γ -M direction than in the Γ -X direction. The reason for this difference between the Γ -M and Γ -X direction will be discussed later.

The data for sample No. 2, which exhibited localized single-particle states in the electrical resistivity, are illustrated in Fig. 4. These spectra are qualitatively different from those of the pure material. Along both symmetry directions we only observe the decaying background of the valence band and a Fermi edge. At no angle is there a maximum indicating a dispersing bandlike state. Considering our signal-to-noise ratio, this implies a reduction of the bandlike states by more than 80%. However, we still observe a Fermi edge with an intensity comparable to that in the pure sample [Fig. 2(a) and 2(b)].

The observation of a reduction of the dispersing states is consistent with the concept of spectral weight shifting from the dispersing bandlike state into an incoherent background of states elastically scattered by impurities. When the single-particle states become localized in real space due to disorder, the wave vector \mathbf{k} is no longer a good quantum number.

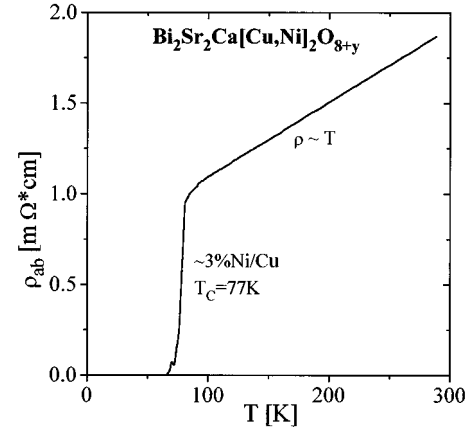


FIG. 5. Electrical a,b -plane resistivity of a Ni-doped Bi-2212 single crystal. This sample shows a very high residual resistivity of $\rho_0 \sim 680 \mu\Omega \text{ cm}$ and T_c is reduced to $T_c = 77 \text{ K}$.

Therefore, one can no longer observe a dispersing bandlike state in the sample where the single-particle excitations are localized. This is the third characteristic feature of spatial localization through disorder. It is worth pointing out that in a conventional metal such as Cu doping at the level of 1% does not have any influence on the strength of the dispersing electronic states.

C. Comparison to Ni doping

In the previous chapter we showed resistivity measurements and ARUPS data for pure and Co-doped Bi-2212. It was shown that the Co doping leads to a metal insulator and to the suppression of dispersing states. In this chapter we present similar data for Ni-doped samples and show that the observed correlation between transport and spectroscopic data is quite general.

Figure 5 shows the resistivity data for a Ni-doped sample. As in the case of Co doping the Ni doping causes a rise of the residual resistivity ($\rho_0 \sim 680 \mu\Omega \text{ cm}$) and a suppression of the superconducting transition temperature ($T_c = 77 \text{ K}$). At high temperature we still observe a linear temperature dependence of the resistivity. This behavior is very similar to that found for the first Co-doped sample No. 1 in Fig. 1.

For the Ni-doped samples we did not succeed in measuring photoemission spectra and resistivity on identical samples. Thus Fig. 6 shows data from a different crystal but from the same batch. The polarization and incidence angles are identical to those for the Co samples. While Fig. 6(a) shows the spectra taken with the photoelectron momentum along Γ -X, 6(b) shows spectra taken along Γ -M (Cu-O-Cu bond direction).

We first compare the spectra for this Ni-doped sample to those of the pure material in Fig. 2. Again we find a decaying background coming from the valence band and a Fermi edge in all spectra. Comparing the spectra at $\theta=8^\circ$ and $\theta=12^\circ$ one finds a dispersing state of weak intensity. Its intensity is even weaker at $\theta=14^\circ$ and it is unobservable at $\theta=16^\circ$. This is consistent with a band crossing around $\theta=14^\circ$, the value where the band was observed to cross E_F in the pure sample. Along the Γ -M direction there is a weak dispersing state moving to E_F as the angle is increased from $\theta=8^\circ$ to $\theta=14^\circ$. Along this direction the intensity of the band state is weak

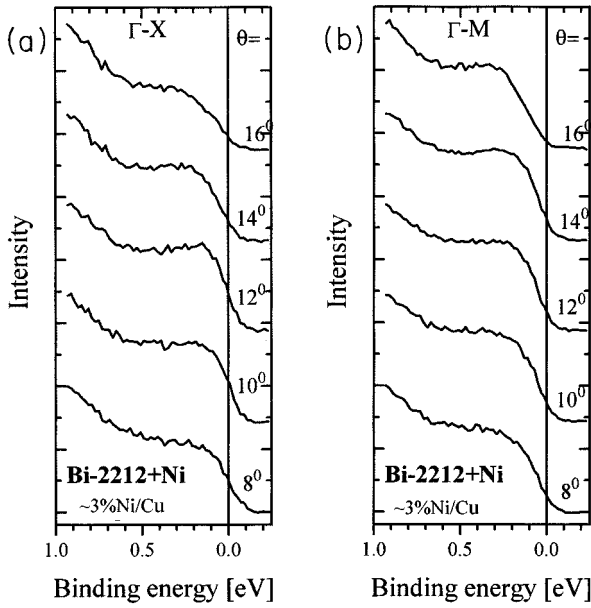


FIG. 6. ARUPS spectra for a Ni-doped Bi-2212 sample. The orientation is identical to that in Fig. 2. This sample shows a reduction of the dispersing state similar to that of the Co-doped (sample No. 1) in Fig. 3.

already in the pure material [Fig. 2(b)]. In this Ni-doped sample it is too weak to draw any quantitative conclusions.

These results are very similar to those observed for the Co-doped sample No. 1. Both show a significant reduction in the intensity of the dispersing state but no visible change in the crossing point or the dispersion. Similar results have also been reported by Gu *et al.* on Zn-doped $\text{YBa}_2\text{Cu}_3\text{O}_{7-\delta}$.⁴³

DISCUSSION

A. Doping-induced disorder as the cause for spatial localization

Any model attempting to explain the effects described in the previous section will have to account for the following facts: The large effects of transition-metal doping on both the resistivity in the normal state and the superconducting transition temperature, the abrupt changes in the ρ_0 and T_c for small changes in the dopant level, and the disappearance of the dispersing state in photoemission. It should also account for the fact that very similar effects have been reported for doping with nonmagnetic Zn (Ref. 3) and for $\text{YBa}_2\text{Cu}_3\text{O}_{7-\delta}$ disordered by ion irradiation.¹⁷ We will show that spatial localization of the conduction electron states through disorder provides such an explanation.

Isolated doped Co atoms locally perturb the electrostatic potential seen by the conduction electrons. This leads to scattering and a finite mean free path λ . The scattering can be treated by the partial wave method. In this case the increase of the residual resistivity $\Delta\rho_0$ caused by an impurity concentration c is given by⁴⁴

$$\Delta\rho_0 = c \frac{4\pi\hbar}{e^2 k_F} \sum_{l=1}^{\infty} l \sin^2(\eta_{l-1} - \eta_l). \quad (1)$$

The scattering can happen in channels which different angular momentum l . These channels are associated with different phase shifts η_l . The phase shifts are related to the charge of the impurity by the Friedel sum rule

$$Z = \frac{2}{\pi} \sum_l (2l+1) \eta_l. \quad (2)$$

This can be used to calculate the maximum possible scattering of such an isolated impurity, the unitary limit $\Delta\rho_u$. It is given by pure s -wave scattering ($l=0$, $\eta_0 = \pi/2$),

$$\Delta\rho_u = c \frac{4\pi\hbar}{e^2 k_F}. \quad (3)$$

Because the scattering processes are assumed to be independent, $\Delta\rho_u$ is linear in the impurity concentration c . To obtain an estimate for the unitary limit in HTSC we use the Fermi momentum given by the crossing of the band state along the Γ - X direction which was shown in Fig. 2(a). Using this value of $k_F = 0.58 \text{ \AA}^{-1}$ we obtain $\Delta\rho_u \sim 9 \times 10^{-4} \Omega \text{ cm}^* c$, or $9 \mu\Omega \text{ cm}$ per percent impurity. This value is only slightly higher than the experimental value found for impurities in Cu metal.⁴⁵ For sample No. 1 with 1.57% Co this would predict a residual resistivity of $\sim 14 \mu\Omega \text{ cm}$. Even for sample No. 1 this unitary limit is a factor of 3 smaller than the experimental value of $\rho_0(\text{No. 1}) = 43 \mu\Omega \text{ cm}$.

Because the Co concentration in sample No. 2 is only slightly higher [$c_{\text{Co}}(\text{No. 2}) = 1.60\%$], Eq. (3) predicts a very similar value in apparent discrepancy with the experimental value of $\rho_0(\text{No. 2}) \sim 600 \mu\Omega \text{ cm}$. This high value can thus not be explained by independent scattering events from individual Co impurities. Even if every Co impurity would cause the maximum possible scattering (unitary limit), as assumed in Eq. (3), this would not suffice to explain the value of the residual resistivity. The maximum possible value of the residual resistivity would be reached for 50% Co for Cu doping ($c=0.5$) because here the disorder is at a maximum. Even such a high Co concentration would only result in a residual resistivity of $\rho_u = 450 \mu\Omega \text{ cm}$. The same argument applies to the Ni-doped sample. Here too, the assumption of scattering from independent impurities is insufficient to explain the observed residual resistivity. Thus this high residual resistivity and the very large change for a minute change in the Co concentration indicate, that the increase of the resistivity is through a cooperative mechanism.

Next we consider the influence of scattering on the ARUPS spectra. The impurity scattering induces transitions from initial eigenstates of the system $|\psi_i\rangle$ to final states $\langle\psi_f|$. The transition probability p is given by Fermi's golden rule,

$$p = \pi/(2\hbar) |\langle\psi_f|V_{\text{imp}}|\psi_i\rangle|^2 n(\psi_f) \quad (4)$$

where V_{imp} is the impurity potential and $n(\psi_f)$ is the density of final states. Because the scattering probability p is proportional to the density of final states, transitions are more likely to occur into regions where this density of states is higher.⁴⁶ For the Bi-2212 system this is the Cu-O-Cu bond direction, where there is an extended singularity,^{39,40} which leads to a high density of states. Thus the impurities should have only little influence in this direction, while they should have significant influence in other directions. This is in agreement

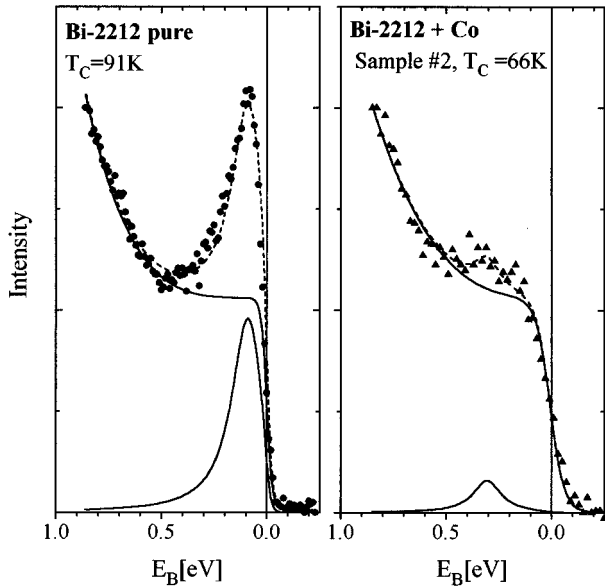


FIG. 7. Decomposition of ARUPS spectra for a pure sample [Fig. 2(a)] and the Co-doped sample No. 2 [Fig. 4(a)]. The three contributions are a dispersing state of Lorentzian shape, a background coming from the valence band (located around $E_B=3$ eV), and a constant term caused by elastic scattering. Full symbols are data points, dashed lines are the fit and solid lines show the individual contributions. In the Co-doped sample (No. 2) the intensity of the dispersing state is reduced by at least a factor of 5.

with the observation that the reduction of the dispersing state is much stronger along the Γ -X direction. In the ARUPS spectra the scattered states will form a constant background which is cut off at E_F by the Fermi-Dirac distribution function. Figure 7 shows how the spectra can be decomposed into a band state and a background. Shown are two spectra taken along the Γ -X direction at an angle of $\theta=12^\circ$ for the pure sample and the Co-doped sample No. 2. The experimental data are shown by full symbols. The dashed lines show a fit to the data. For this fit a dispersing state of Lorentzian shape and a background I_{BG} consisting of a constant term plus a power law [$I_{BG}(E)=a+b^*E_b^3$] was assumed. The spectrum is cut off by a Fermi-Dirac distribution function. The solid lines show the dispersing state and the background contribution, respectively. The fit follows the experimental data quite well.

For the pure sample there is a well-defined dispersing band state of width $W=0.19$ eV and binding energy $E_B=0.09$ eV. The dispersing state and the constant background term are of almost equal intensity at the Fermi level. For the Co-doped sample No. 2, which exhibited the insulating upturn in the resistivity, the dispersing state is virtually absent. A least-squares fit results in a dispersing state of width $W\sim 0.2$ eV and binding energy $E_B\sim 0.2$ eV. Its intensity is less than 15% of the constant background. Because of its weak intensity the values for both the width and the binding energy have large uncertainties in this sample.

This analysis shows that spectral weight has been transferred from the dispersing band state in the pure sample to a constant background in the Co-doped sample. A quantitative analysis of this shift of spectral weight is not possible be-

cause it is not clear how to normalize the spectra. The reason is that the band structure is strongly anisotropic^{39,40} and the scattering is proportional to the final density of states. Thus a conservation of spectral area for a given direction in the Brillouin zone cannot be expected.

As outlined above spatial localization through strong disorder scattering can explain the data on the electrical resistivity and the angle-resolved photoemission presented in this paper. It also provides an explanation for the similarity of the data shown here with data on Zn-doped samples³ and on ion irradiated samples.¹⁷

Alternative explanations include Abrikosov-Gor'kov pair breaking,⁷ a Kondo-type scattering effect⁴⁷ or a Mott transition.³⁶ However none of these provides a consistent explanation for all of the data. Abrikosov-Gor'kov pair breaking would affect the superconducting transition temperature T_c but would neither affect the resistivity above T_c nor the intensity of the dispersing band states. This is in clear contradiction to the experimental data presented here and in previous work.^{3,48} In case of a Kondo effect neither nonmagnetic Zn doping nor ion irradiation should have any effect because both produce nonmagnetic defects. Both Abrikosov-Gor'kov scattering and a Kondo effect assume independent scattering events and are thus unable to explain the residual resistivity exceeding the unitary limit by as much as a factor of 40. A Mott-type transition would imply that the carrier density changes and that below a certain carrier density the hybridization between carriers becomes so small that they are localized on a single atom. Experimentally, we observe no change in the Fermi surface crossing (k_F) and previous work also indicates little or no change in the Hall effect.^{3,17} Both facts argue against a changing carrier concentration and thus against a Mott transition. The standard weak localization process through quantum interference¹⁶ of elastically scattered waves can also be excluded because the magnetic moment of the Co and Ni atoms breaks time-reversal symmetry and destroys the quantum interference.

The effect of the metal-insulator transition on the band structure has previously been studied by Rong Liu and co-workers for $YBa_2Cu_3O_x$ with $6.3\leq x\leq 6.9$.^{29,30} These authors did not consider the possibility of spatial localization. In their experiment the change in the oxygen content is expected to change the volume of the Fermi surface. In contrast to this our experiment leaves the carrier density constant and is thus not expected to affect the volume of the Fermi surface. The experimental findings are similar in both cases. For metallic samples dispersing states are observed. Within the experimental error their band crossings are identical to those of the pure material. For insulating samples one observes a very significant reduction of the spectral weight for these dispersing states. Apparently the main effect in both cases is the destruction of the periodic potential leading to spatial localization, an idea we have introduced in this paper. A change of the volume of the Fermi surface is too small to be detected experimentally. For the Co- and Ni-doped Bi-2212 discussed here the disorder, caused by the substitution of Co and Ni for Cu in the CuO_2 plane, is apparent. In the case of the $YBa_2Cu_3O_x$ the disorder is probably caused by changes in the a - and b -lattice constant which accompany the random oxygen vacancies in the Cu-O chains.

B. Coexistence of spatial localization and superconductivity

As shown in Figs. 1 and 4 sample No. 2 exhibits an increase in the electrical resistivity below $T_{\min}=190$ K, caused by localization of the carriers, and a superconducting transition at $T_c=66$ K. Consequently the Cooper pairs forming the superconducting state must be composed of spatially localized single-particle states. Such a coexistence of localization and superconductivity is very unusual. Experimentally, it has only been observed in granular systems such as Al:Ge (Ref. 13) and In:O.²¹ Theoretically, it has been studied by several authors^{22–25} who demonstrated that localization and superconductivity are not mutually exclusive. Anderson's theorem is still valid in a narrow region on the insulating side of the superconductor-insulator transition.^{22,23} In the localized region of the insulator-superconductor transition the density of states can no longer be approximated by a spatial average, but must be considered a local quantity $N(E,r)$. Ma and Lee²² showed that a superconducting wave function can be formed provided there are several localized states within an energy range equal to the superconducting gap Δ_0 of the material,

$$a_H^d \Delta_0 \langle N(E_F, r) \rangle \gg 1. \quad (5)$$

Here d is the dimension, Δ_0 is the superconducting gap, and $\langle N(E_F, r) \rangle$ denotes the density of localized electronic states averaged over an energy region of the size Δ_0 . We can use this to discuss the hierarchy of length scales involved in the problem. For this we assume the extreme atomic limit where the carriers do not interact. This assumption ignores hybridization between the carriers, which is certainly non-negligible and which will lead to a larger value for the localization radius. Neglecting hybridization effects the normal state is governed by the separation between two carrier states d_{e-e} and the localization radius. In the two-dimensional CuO_2 plane the carrier separation is given by $d_{e-e} = a/(c^{1/2})$ where $a=5$ Å is the lattice constant and c the carrier concentration. In order for localization to occur the separation between two carriers d_{e-e} has to be larger than their spatial extent a_H , or $d_{e-e} > a_H$. This argument is equivalent to the Joffe-Regel ($k_F^* \lambda = 1$) criterion for localization in materials with one carrier per atom.³⁶ In this case the transport will happen through thermally activated hopping between different carrier sites leading to a negative temperature coefficient of the resistivity ($d\rho/dT < 0$). Superconductivity, on the other hand, can only occur when there are at least two carriers per coherence volume or, $\xi_{ab} > d_{e-e}$. Thus in the absence of hybridization coexistence of localization and superconductivity requires

$$\xi_{ab} > d_{e-e} > a_H. \quad (6)$$

In Bi-2212 the in-plane coherence length is estimated to be around $\xi_{ab} \sim 10\text{--}20$ Å. The carrier concentration is about $c=0.15$ carriers per Cu leading to a carrier separation of $d_{e-e} = 5 \text{ Å} * (0.15^{-1/2}) \sim 13$ Å. In agreement with the argument above the coherence length is thus larger than the carrier separation, but only by a surprisingly small amount. How

superconductivity can work with such a small number of carriers per coherence volume is a puzzling feature of high-temperature superconductivity. This argument leads to an upper bound for the localization radius a_H . According to Eq. (6), a_H has to be smaller than the carrier separation for the coexistence of localization and superconductivity. Thus it has to be smaller than about $a_H < 13$ Å. The carriers are thus localized in an area corresponding to $n < (a_H/a)^2 \sim 6$ Cu atoms. Such a value seems reasonable because it is intermediate between the completely delocalized Bloch state ($a_H = \infty$) and localization on a single atomic site. It means a carrier is only shared between a Cu atom and its nearest neighbors.

The work of Ma and Lee²² can now be used to estimate the width of the region where localization and superconductivity coexist. Taking the localization length on the insulating side of the superconductor-insulator transition from scaling theory they estimated the width of the coexistence region $(n_c - n)/n_c$ as

$$(1 - n/n_c)^\nu \sim (E_F/\Delta)^{1/d}. \quad (7)$$

Here d is the dimensionality, n_c is the critical concentration for the superconductor-insulator transition, and ν is the critical exponent. Assuming $d=2$ and taking $\nu=-1$ (Ref. 5) and values of $E_F \sim 400$ meV and $\Delta \sim 16$ meV,⁴⁹ we obtain a coexistence region of $(1 - n/n_c) \sim 20\%$. Using the value of $n_c = 1.6$ at. % for the critical concentration in the case of Co doping this yields a coexistence region of only ~ 0.3 at. % Co. The relative width of $(1 - n/n_c) \sim 20\%$ is a factor of 2 larger than that of classical low-temperature superconductors where Ma and Lee estimated it to be $\sim 10\%$.²² Although both the larger gap Δ_0 and the lower Fermi energy E_F in HTSC favor the coexistence of localization and superconductivity, these effects are partially canceled by the lower dimensionality $d=2$ as compared to $d=3$ in the granular systems. The narrow coexistence region is consistent with our observation that sample No. 1 and sample No. 2 have very similar Co contents (1.57 at. % and 1.60 at. %, respectively) but very dissimilar properties.

CONCLUSIONS

We have shown that in addition to causing a metal-insulator transition in the resistivity, transition-metal doping causes a suppression of the dispersing electronic states as observed by angle-resolved photoemission. We have shown that many experimental facts can be understood by assuming spatial localization of the conduction electrons by scattering from disorder caused by the doped impurities.

However the origin of such localization remains unclear. Our data indicate scattering from Co impurities as high as a factor of 40 higher than the unitary limit. Thus the scattering has to be a cooperative effect, which excludes both standard Abrikosov-Gor'kov and Kondo scattering which are single-ion effects. On the other hand, quantum interference effects as in weak localization theory can be excluded because of the local magnetic moment of the Co and the Ni, which destroys the interference. While transport experiments on samples

with intentionally increased disorder show all characteristics of a homogenous system,^{17,3} photodoping experiments show the characteristics of a granular system.^{18,37} This disagreement underlines the fundamental lack of understanding for the localization mechanism taking place in the cuprates.

Lastly, it is unclear why we observe superconductivity with a transition temperature of $T_c \sim 66$ K (about two thirds of the pure T_c) for a sample where the resistivity and the ARUPS data indicate that the conduction electrons are spatially almost localized. It shows that the superconducting pairing attraction is nearly equally effective for spatially localized as for delocalized carriers. This fact must be addressed by theories attempting to explain the microscopic mechanism in the cuprates.

ACKNOWLEDGMENTS

It is our pleasure to thank Hans Kroha, Robert Dynes, Allen Goldmann, and Bernd Beschoten for helpful discussion. The staff of SRC, especially Roger Hansen, was of great help. We would like to thank Lazlo Forro for his help during the resistivity measurements as well as G. Burri and G. Trolliet for performing the microprobe analysis. This work was supported by the National Science Foundation both directly and indirectly through the support of the Synchrotron Radiation Center, by the Deutsche Forschungsgemeinschaft under Grant No. Qu72/2-2, by Fonds National Suisse de la Recherche Scientifique, and by Ecole Polytechnique Fédérale de Lausanne.

-
- *Present address: Experimentalphysik 10.2, Universität des Saarlandes, Im Stadtwald, Bau 22-2.08, D-66041 Saarbrücken, Germany.
- ¹J. G. Bednorz and K. A. Müller, *Z. Phys. B* **64**, 189 (1986).
 - ²K. Kitazawa, in *Earlier and Recent Aspects of Superconductivity*, edited by J. G. Bednorz and K. A. Müller, Springer Series in Solid State Sciences, Vol. 90 (Springer-Verlag, Berlin, 1990), p. 45.
 - ³A. Maeda, T. Yabe, S. Takebayashi, M. Hase, and K. Uchinokura, *Phys. Rev. B* **41**, 4112 (1990), and references therein.
 - ⁴M. Z. Cieplak, S. Guha, H. Kojima, P. Lindendorf, G. Xiao, J. Q. Xiao, and C. L. Chien, *Phys. Rev. B* **46**, 5535 (1992).
 - ⁵C. Quitmann, D. Andrich, C. Jarchow, M. Fleuster, B. Beschoten, G. Güntherodt, V. V. Moshchalkov, G. Mante, and R. Mantske, *Phys. Rev. B* **46**, 11 813 (1992).
 - ⁶A. A. Abrikosov and L. P. Gor'kov, *Zh. Eksp. Teor. Fiz.* **35**, 1558 (1950); *Sov. Phys. JETP* **8**, 1090 (1959).
 - ⁷K. Maki, in *Superconductivity*, edited by R. D. Parks (Dekker, New York, 1969), Vol. 2.
 - ⁸P. W. Anderson, *J. Phys. Chem. Solids* **11**, 26 (1959).
 - ⁹D. B. Haviland, Y. Liu, T. Wang, and A. M. Goldman, *Physica B* **169**, 238 (1991), and references therein.
 - ¹⁰R. C. Dynes, R. P. Barber, Jr., and F. Sharifi, in *Ordering Disorder, Prospect and Retrospect in Condensed Matter Physics*, edited by Vipin Srivastava, Anil K. Bhatnagar, and Donald G. Nangle, AIP Conf. Proc. No. 286 (AIP, New York, 1993), pp. 96–108. See also other contributions to this proceeding.
 - ¹¹J. M. Valles, Jr., Shih-Ying, R. C. Dynes, and J. P. Grano, *Physica C* **197**, 522 (1994).
 - ¹²J. M. Valles, Jr., R. C. Dynes, and J. P. Garno, *Phys. Rev. B* **40**, 6680 (1989).
 - ¹³Y. Shapira and G. Deutscher, *Phys. Rev. B* **27**, 4463 (1990).
 - ¹⁴R. C. Dynes, A. E. White, J. M. Graybeal, and J. P. Garno, *Phys. Rev. Lett.* **57**, 2195 (1986).
 - ¹⁵D. B. Haviland, Y. Liu, and A. M. Goldman, *Phys. Rev. Lett.* **62**, 2180 (1989).
 - ¹⁶For a review, see, B. Kramer and A. MacKinnon, *Rep. Prog. Phys.* **56**, 1469 (1993).
 - ¹⁷J. M. Valles, Jr., A. E. White, K. T. Short, R. C. Dynes, J. P. Garno, A. F. J. Levi, M. Anzlowar, and K. Baldwin, *Phys. Rev. B* **39**, 11 599.
 - ¹⁸G. Yu, C. H. Lee, D. Mihailovic, A. J. Heeger, C. Fincher, N. Herron, and E. M. McCarron, *Phys. Rev. B* **48**, 7545 (1993).
 - ¹⁹Gang Xiao, M. Z. Cieplak, D. Musser, A. Gavrin, C. Fincher, N. Herron, and E. M. McCarron, *Phys. Rev. B* **48**, 7545 (1993).
 - ²⁰B. vom Hedt, W. Lissek, K. Westerholdt, and H. Bach, *Phys. Rev. B* **49**, 9898 (1994).
 - ²¹D. Shahar and Z. Ovadyahu, *Phys. Rev. B* **46**, 10 917 (1992).
 - ²²Michael Ma and Patrik A. Lee, *Phys. Rev. Lett.* **32**, 5658 (1985).
 - ²³L. N. Bulaevskii and M. V. Sadovskii, *J. Low Temp. Phys.* **59**, 85 (1985).
 - ²⁴A. Kapitulnik and G. Kotliar, *Phys. Rev. Lett.* **54**, 473 (1985).
 - ²⁵A. Kapitulnik and G. Kotliar, *Phys. Rev. B* **33**, 3146 (1986).
 - ²⁶L. Coffey and D. L. Cox, *Phys. Rev. B* **37**, 3389 (1988).
 - ²⁷G. Kotliar and C. M. Varma, *Physica A* **167**, 288 (1990).
 - ²⁸Patrik A. Lee, *Phys. Rev. Lett.* **71**, 1887 (1993).
 - ²⁹Rong Liu, B. W. Veal, A. P. Paulikas, J. W. Downey, H. Shi, C. G. Olson, C. Gu, A. J. Arko, and J. J. Joyce, *Phys. Rev. B* **45**, 5614 (1992).
 - ³⁰Rong Liu, B. W. Veal, A. P. Paulikas, J. W. Downey, P. J. Kostic, S. Fleshler, U. Welp, C. G. Olson, X. Wu, A. J. Arko, and J. J. Joyce, *Phys. Rev. B* **46**, 11 056 (1992).
 - ³¹M. D. Kirk, J. Nogami, A. A. Baski, D. B. Mitzi, A. Kapitulnik, T. H. Geballe, and C. F. Quate, *Science* **242**, 1673 (1988).
 - ³²S. A. Sunshine, L. F. Schneemeyer, D. M. Murphy, R. J. Cava, B. Batlogg, R. B. van Dover, R. M. Fleming, S. H. Glarum, R. Farrow, J. J. Krajewski, S. M. Zahurak, J. V. Waszczak, J. H. Marshall, P. Marsh, L. W. Rupp, Jr., and W. F. Peck, *Phys. Rev. B* **38**, 893 (1988).
 - ³³J. M. Tarascon, Y. Le Page, P. Barboux, B. G. Bagley, L. H. Greene, W. R. McKinnon, G. W. Hull, M. Giroud, and D. W. Hwang, *Phys. Rev. B* **37**, 9382 (1988).
 - ³⁴R. J. Kelley, Jian Ma, M. Onellion, Phillipe Almeras, H. Berger, and G. Margaritondo, *Phys. Rev. B* **48**, 3534 (1993).
 - ³⁵M. Gurvich and T. Fiory, *Phys. Rev. Lett.* **59**, 1337 (1987).
 - ³⁶N. F. Mott, *Metal-Insulator Transitions* (Taylor and Francis, London, 1974).
 - ³⁷G. Yu, C. H. Lee, A. J. Heeger, N. Herron, E. M. McCarron, Lin Cong, G. C. Spalding, C. A. Nordman, and A. M. Goldman, *Phys. Rev. B* **45**, 4964 (1992).
 - ³⁸Alan J. Heeger and Gang Yu, *Phys. Rev. B* **48**, 6492 (1993).
 - ³⁹D. S. Dessau, Z.-X. Shen, D. M. King, D. S. Marshall, L. W. Lombardo, P. H. Dickinson, A. G. Loeser, J. DiCarlo, C.-H. Park, A. Kapitulnik, and W. E. Spicer, *Phys. Rev. Lett.* **71**, 2781 (1993).
 - ⁴⁰Jian Ma, C. Quitmann, R. J. Kelley, P. Almeras, H. Berger, G. Margaritondo, and M. Onellion, *Phys. Rev. B* **51**, 3832 (1995).

- ⁴¹J. C. Campuzano, K. Gofron, H. Ding, R. Liu, B. Dabrowski, and B. J. W. Veal, *J. Low Temp. Phys.* **95**, 245 (1994).
- ⁴²A. A. Abrikosov, J. C. Campuzano, and K. Gofron, *Physica C* **214**, 73 (1994).
- ⁴³Chun Gu, B. W. Veal, R. Liu, H. Ding, A. P. Paulikas, J. C. Campuzano, P. Kostic, R. W. Wheeler, and H. Zhang, *J. Phys. Chem. Solids* **54**, 1177 (1993).
- ⁴⁴See, for example, C. Kittel, *Quantum Theory of Solids* (Wiley, New York, 1987).
- ⁴⁵For a discussion, see, J. M. Ziman, in *Electrons and Phonons* (Clarendon, Oxford, 1960).
- ⁴⁶A. A. Abrikosov, *Physica C* **244**, 243 (1995).
- ⁴⁷See, for example, G. Grüner and A. Zawadowski, *Rep. Prog. Phys.* **7**, 1497 (1974).
- ⁴⁸B. Jayaram, P. C. Lanchester, and M. T. Weller, *Phys. Rev. B* **43**, 10 589 (1991).
- ⁴⁹R. J. Kelley, Jian Ma, C. Quitmann, G. Margaritondo, and M. Onellion, *Phys. Rev. B* **50**, 590 (1994).